DOI:10.22337/2587-9618-2024-20-3-14-23

DEFORMATION MODELING OF ROD STRUCTURES UNDER KINEMATIC CONTROLLED ACTION

Peter P. Gaydzhurov [1], ***Nadezhda G. Tsaritova*** [2]

[1] Don State Technical University, Rostov-on-Don, RUSSIA

[2] Platov South-Russian State Polytechnic University, Novocherkassk, RUSSIA

Abstract. Currently, transformable rod systems have found wide application in the designs of spacecraft panels and as various stents in medicine. It is of some theoretical interest to extent the idea of geometric variability to spatial rod systems of complex shape. The concept of kinematic shaping of a regular rod system from a flat to a domed position is proposed. The finite element method in combination with the modified Lagrange method was used for numerical implementation of this concept. To assess the level of deformed state of the rods of a modular lattice, an energy criterion is proposed that allows determining the most loaded rods considering genetic nonlinearity of the system.

Keywords: deformation modeling, rod system, finite element method, modified Lagrange method, genetic nonlinearity

ДЕФОРМАЦИОННОЕ МОДЕЛИРОВАНИЕ СТЕРЖНЕВЫХ КОНСТРУКЦИЙ ПРИ УПРАВЛЯЕМОМ КИНЕМАТИЧЕСКОМ ВОЗДЕЙСТВИИ

П.П. Гайджуров [1], ***Н.Г. Царитова*** [2]

[1] Донской государственный технический университет, г. Ростов-на-Дону, РОССИЯ

[2] Южно-Российский государственный политехнический университет (НПИ) имени М.И. Платова, г. Новочеркасск, РОССИЯ

Аннотация. В настоящее время трансформируемые стержневые системы нашли широкое применение в конструкциях панелей космических аппаратов и медицине в виде различных стентов. Представляет определенный теоретический интерес развить идею геометрической изменяемости на пространственные стержневые системы сложной формы. Предлагается концепция кинематического формоизменения регулярной стержневой системы из плоского в куполообразное положение. Для численной реализации применен метод конечных элементов в сочетании модифицированным методом Лагранжа. Для оценки уровня деформированного состояния стержней регулярной решетки с учетом генетической нелинейности предложен энергетический критерий, позволяющий определить наиболее нагруженные стержни.

Ключевые слова: деформационное моделирование, стержневая система, метод конечных элементов, модифицированный метод Лагранжа, генетическая нелинейность

INTRODUCTION

Deformation modeling appeared as one of the directions of computer graphics, which allows to convert the kinematics of a physically observed object into virtual reality. The concept of a deformable model is usually considered from the point of view of mechanics of a deformable solid. In accordance with this concept, it is convenient to describe the deformation process of some continuum in Lagrangian coordinates. The paradigm of the deformable model is a “snake”, the shape and geometry of the “body” of which depends on the displacements of key points [1, 2, 3]. Formally, a “snake” is a contour defined parametrically, as a rule, by a cubic spline. The technology of approximation of the initial contour by a spline is based on the procedure of minimization of the functional associated with the deformation energy of the contour within the boundaries of the area surrounding each key point (Fig. 1).

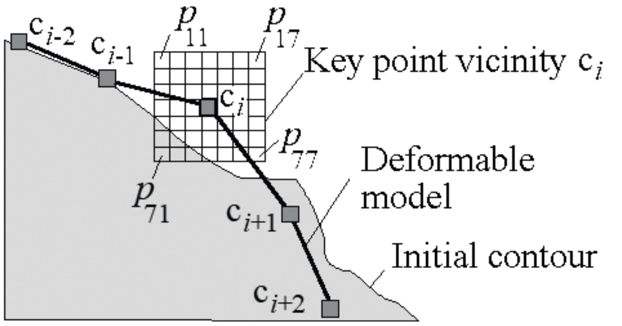

Figure 1. Deformable "snake" model

Approximation of the initial contour with a "snake"-type deformable model is widely used in biomedical research such as "computed tomography", as well as in applications of artificial intelligence to motion tracking and object identification tasks.

Another approach to the construction of a geometrically deformable model (GDM) is the concept based on the expansion of a virtual thin-walled balloon inside the boundaries of the scanned object (Fig. 2). The GDM technology uses the finite element method in the form of the displacement method as a mathematical apparatus. The balloon is modeled by momentless three-node plate finite elements. The geometry of the balloon at time t is represented in parametric form [4, 5]:

$$R(u,v,t)=\left[\psi_x(u,v,t),\psi_y(u,v,t),\psi_z(u,v,t)\right],$$

where ψ_x, ψ_y, ψ_z are approximating cubic spline functions along the axes x, y, z; u, v are dimensionless variables such that $u\in[0,1]$, $v\in[0,1]$. During the scanning of the internal cavity of the object under study, each node of the finite element model is attracted to a point of the bounding contour in the normal direction (Fig. 3). The current deformed state of the finite element is fully determined by the metric tensor [6, 7, 8]

$$g\left(R(u,v,t)\right)=\frac{\partial R}{\partial u}\frac{\partial R}{\partial v}.$$

The fundamental theorem of the mechanics of a deformable solid [9] stipulates that two bodies in Euclidean space will have the same instantaneous shape, i.e., differ only in displacement as a "rigid whole", if their metric tensors are identical at time t.

Figure 2. Visualization of GDM technology [6]

Figure 3. Balloon model deformed by a point force [7]

According to [6], the adaptation algorithm is constructed in such a way that the following condition is satisfied at each step in the nodes of the finite element mesh:

$$\begin{aligned}C(x,y,z)=\alpha_0 D(x,y,z)+\alpha_1 I(x,y,z)\\+\alpha_2 T(x,y,z)\geq 0\end{aligned},\qquad(1)$$

where $C(x,y,z)$ is a target function associated with the current position of the model node point; $D(x,y,z)$ is the deformation potential (monotonically decreasing or increasing function); $I(x,y,z)$ is a constraint function "informing" a finite element mesh node that it can be in contact with a voxel (an element of the object image); $C(x,y,z)$ is the topological information function, preventing nodes of the finite element model from penetrating the object boundary; α_0, α_1, α_2 are weight factors. Condition (1) causes the model to deform until all vertices reach the boundary of the scanned object.

Another direction of deformation modeling is the analysis of the behavior of spatial rod structures experiencing large linear and angular displacements at small deformations during operation. In this case, the numerical solution of the geometrically nonlinear problem is based on the Newton-Raphson iterative procedure and the method of "corrective arcs", the essence of which is the adaptive adjustment of the loading step value when approaching and after passing the bifurcation point [9,10]. It should be noted that the calculation of the rod system by the finite element method (FEM), taking into account large displacements, uses a tangent stiffness matrix. The construction of this matrix is based on the minimization of the strain energy potential [9]:

$$\frac{\partial^2 U}{\partial \mathbf{y}^2}\Delta\mathbf{y}+\frac{\partial U}{\partial \mathbf{y}}=\mathbf{P}^{(e)},$$

where $\mathbf{y}$, $\mathbf{P}^{(e)}$ are the vectors of displacements and generalized external forces. The potential energy of a finite element (FE) can be represented as

$$U=\frac{1}{2}\mathbf{y}^T\left[k\right]^{(e)}\mathbf{y},$$

where $\left[k\right]^{(e)}$ is the element stiffness matrix in global axes. The paper [11] proposes to consider the matrix elements $\left[k\right]^{(e)}$ to be constant for twice differentiation U.

As an illustration of the solution of such a problem in the geometrically nonlinear formulation, we have considered a test task from [9, 11]. A flexible curvilinear bar of rectangular cross-section of 1×1 m with arch radius of 100 m at central angle of 45^0 is rigidly fixed at the end (x = 0, y = 0, z = 0). It is subjected to bending out of the plane by a concentrated force F_z = 100 N. The coordinates of the free end of the rod in the initial position are [70,71; 70,71; 0] m. Mechanical constants of the rod material: modulus of elasticity E = 10 MPa; Poisson's ratio ν = 0. Fig. 4 shows the results of the analysis performed using the nonlinear solver of the ANSYS software [12]. The beam was divided into 16 spatial beam-type elements of BEAM4.

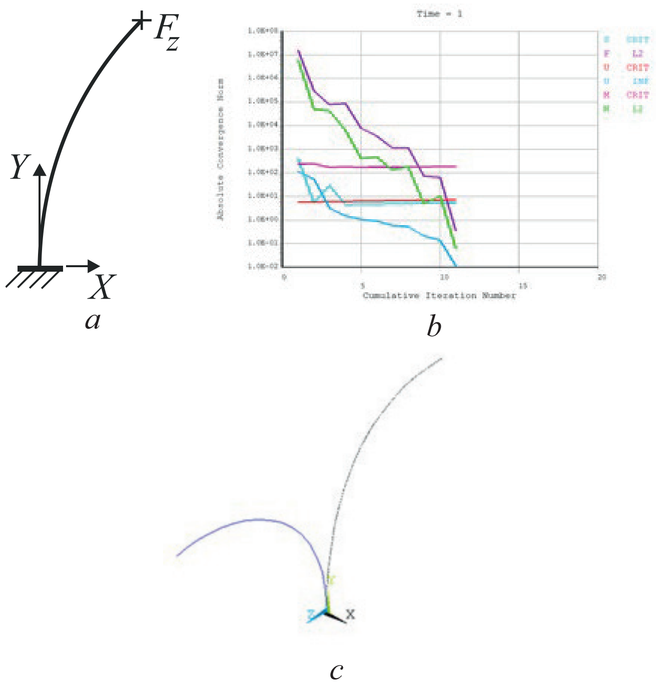

Figure 4. Results of analysis of a curved beam: a - initial state of the beam; b - parameters of ANSYS nonlinear solver; c - visualization of the beam deformation relative to the initial position

The displacement coordinates of the load application point were [46.84; 15.56; 53.66] m according to [9, 11] and [46.9; 15.6; 53.6] m according to the ANSYS solution. As can be seen, the given displacement values are quite close.

The above presented concepts of deformation modeling are highly specialized and cannot be extended to the problems of structural mechanics related to the study of kinematically transformed rod systems. In this regard, the development of a finite element modeling approach for rod structures considering the structural shape change of the initial geometry into some structural state is an urgent problem.

MATERIALS AND METHODS

Let us investigate the regular rod systems shown in the initial (undeformed) state in Fig. 5., taking into account the controlled displacement of contour nodes.

A distinctive feature of these computational schemes from the one presented in [13] is the presence of a nodal platform S modeled by rods with an elastic modulus exceeding the elastic modulus of the connecting rods by five orders of magnitude. From the structural point of view, the introduction of platforms S allows to conventionally account for the nodal connections of real rod systems. In the extracted fragments of Fig. 5, the letters L and B denote the lattices composed of hinged-rod (truss) and beam finite elements, respectively. In both cases, the nodal platforms S are modeled by almost non-deformable beam FE.

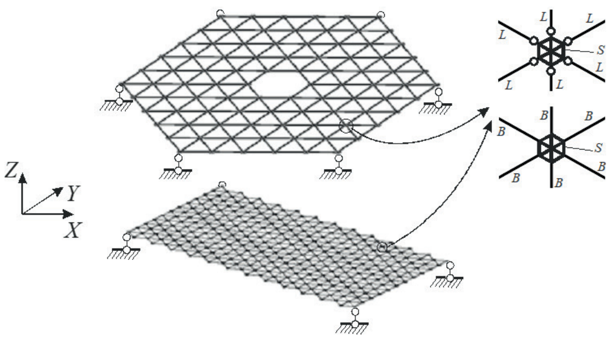

Figure 5. Rod model in the initial state

To investigate the process of change of a rod structure shape, we apply a modified Lagrange method [14], the essence of which consists in a discrete increment of displacements of contour nodes and reconstruction of the finite element mesh geometry in the current initial basis, taking into account the obtained nodal displacements. In the literature on structural mechanics, this type of nonlinearity is called genetic [15]. For program realization of this concept, we use the APDL programming language [12], embedded in the ANSYS Mechanical software package.

At kinematic quasi-static shape change, internal forces caused by gravitational influence and structural bonds will appear in the structure's rods. To assess the level of deformed state of the finite element model, we introduce an energy criterion, which for the adopted scheme of rod discretization can be indirectly represented in the form of longitudinal strain $\varepsilon = \Delta l / l$, where Δl is the changes in the rod length; l is the initial rod length.

RESEARCH RESULTS

First, as an object of study, consider a regular rod system that is hexagonal in plan (Fig. 6). The lengths of the rods forming the regular lattice of the structure are 0.4 m. The radius of the circumscribed circle of the platform S is 0.05 m. The mechanical constants of the rods (aluminum alloy) are $E = 7.2 \cdot 10^4$ MPa, $\nu = 0.32$, specific gravity = 2885 kg/m^3. The rods of the lattice and platforms S have a tubular cross-section with an outside diameter of 18 mm and a wall thickness of 1.5 mm.

Fig. 7 shows the visualization of the first mode of natural vibrations of the model for truss and beam FEs. As can be seen, the regular lattice modeled by truss FEs is kinematically variable, since it allows rotation of rigid platforms. Therefore, in the further study we will use only truss FEs.

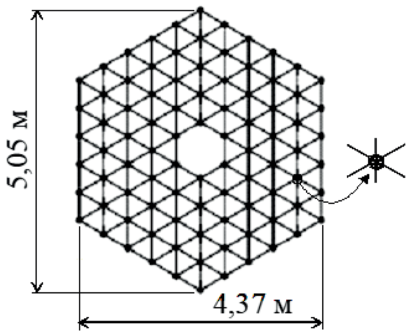

Figure 6. Initial dimensions of the rod structure with hexagonal plan

It should be noted that the transformation process will not lead to the expected lifting of the rod lattice from the position when the coordinates of all nodes $z_i = 0$. Thus, is necessary to "start" the transformation from a pre-prepared dome-shaped geometry (Fig. 8). Let's take the "starting" lifting height of $\Delta u_z = 0.1$ m.

a

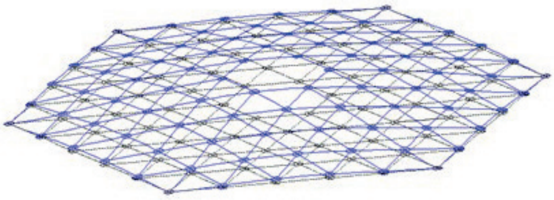

b

Figure 7. The first eigenmode:
a - truss FEs; b - bar FEs

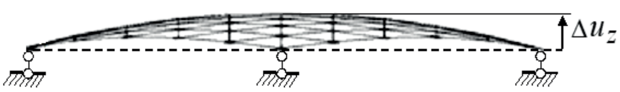

Figure 8. "Start" position of the rod structure

Let us analyze the kinematic change for the considered rod structure in the "starting" position, with discrete displacement of contour nodes in the direction of *X* and *Y* axes (Fig. 9). We assume that the displacement steps and are synchronous Δ_x and Δ_y equal to 0.01 m.

Figure 10 shows a visualization of the shape of the structure after 50 steps. The lift of the center point, when the transformation was completed, was of f_{max} = 0.92 m. Changes $\Delta l / l$ in the rods of the lattice at discrete displacements along the *X* and *Y* axes are plotted in Fig. 11.

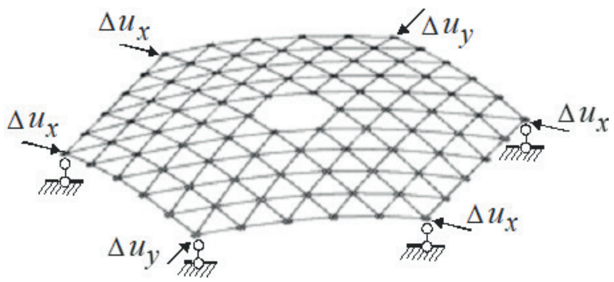

Figure 9. Discrete displacements along the X and Y axes

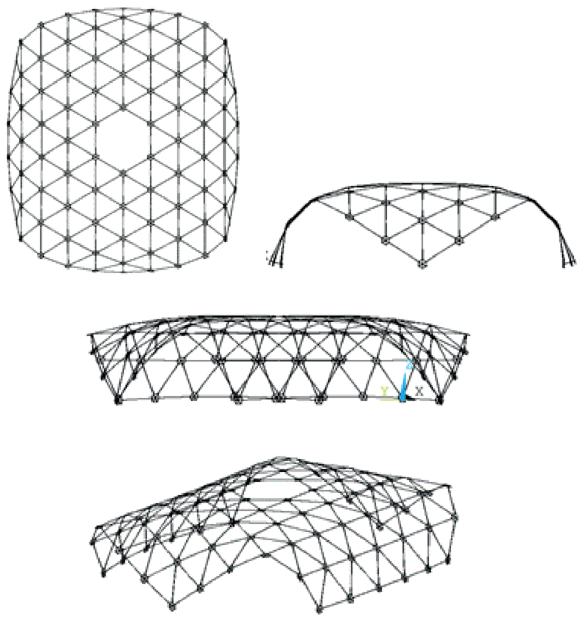

Figure 10. Visualization of a form change after 50 displacement steps along the X and Y axes

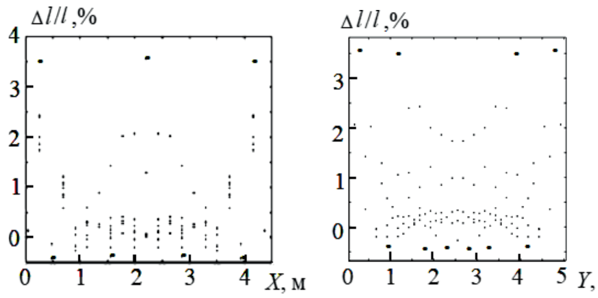

Figure 11. Changes $\Delta l / l$ in the rods at displacement of contour nodes along X and Y axes

Fig. 11 shows that the rods adjacent to the contour nodes will be the most stressed in this transformation scheme. In natural terms, the extreme value $\Delta l / l$ =3.5 % corresponds to the rod elongation Δl = 14 mm.

Fig. 12 shows the results of solving a similar problem using the nonlinear solver of ANSYS Mechanical. In this case, the "starting" position of the lattice was also used and kinematic boundary conditions in the form of displacements of contour nodes equal to 0.5 m were set. The simulation was performed taking into account large displacements (*Large Displacement Static*).

By comparing the patterns of the lattice in the deformed state shown in Figs. 10 and 12, we establish their qualitative agreement.

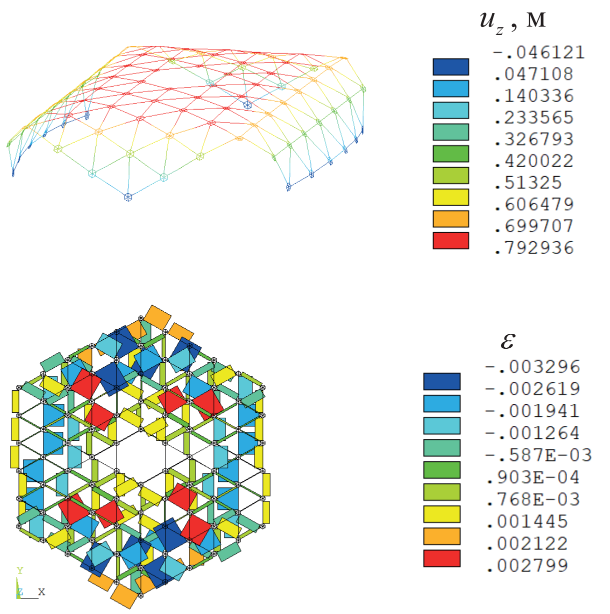

Figure 12. Results of the analysis using a non-linear solver: u_z - vertical displacements; ε – longitudinal strain

At the same time, the value of the maximum lift at one-step transformation is of f_{max} = 0.79 m, which is less than at discrete forming f_{max} = 0.92 m. There is also a significant qualitative and quantitative difference in the distribution patterns of longitudinal strains in the lattice rods. Moreover, at discrete shaping, the extreme value exceeds by more than an order of magnitude the similar value shown in Fig. 12. Thus, the proposed method of discrete shaping combined with step-by-step correction and reconstruction of the finite element mesh taking into account the obtained nodal displacements should be used when modeling the process of transformation of the geometry of a regular lattice system.

Let us consider the scheme of transformation of the rod structure at discrete displacements Δ_x = 0.01 mm along the X axis only (Fig. 13). Visualization of the lattice shape after 50 steps of transformation along X is shown in Fig. 14.

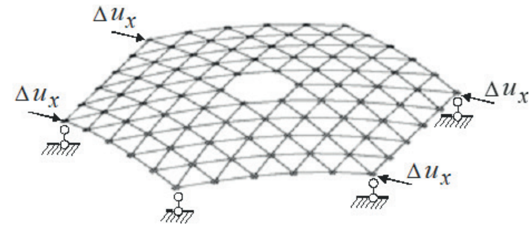

Figure 13. Discrete displacements along the X axis

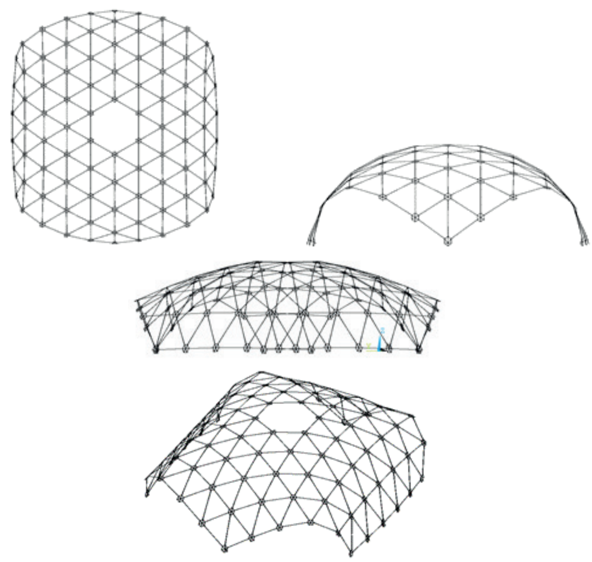

Figure 14. Visualization of the shape change after 50 displacement steps along the X-axis

In this case, the lift at the pole point, when the transformation was completed, was 1.3 m. The corresponding plots of longitudinal strain in the rods are shown in Fig. 15.

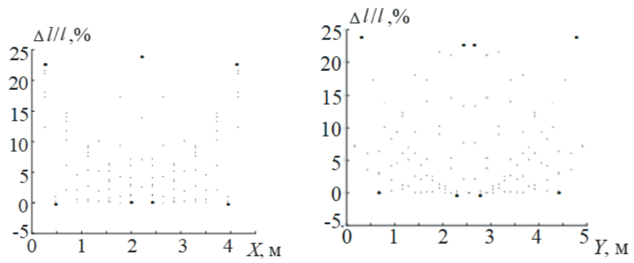

Figure 15. Change $\Delta l / l$ in rods when contour nodes are displaced along the X-axis

Comparing the dome shapes of the rod structure under uniform compression along the X and Y axes (Fig. 10) and compression only in the X

direction (Fig. 14), we conclude that in the second case there is a more pronounced roundness of the surface. At the same time, the maximum value of the ratio $\Delta l / l$ in Fig. 15 is almost seven times greater than the similar value presented in the plots of Fig. 11.

Finally, let us perform deformation modeling of a regular rod system with rectangular plan (Fig. 16). The design scheme for the transformation is shown in Fig. 17. The step Δ_x along the X-axis is assumed to be 0.05 m.

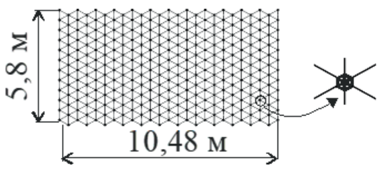

Figure 16. Initial dimensions of the rod rectangular structure

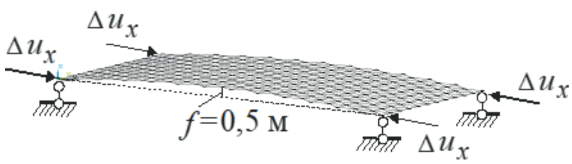

Figure 17. "Start" position of the rod structure

The visualization of the lattice patterns after 50 and 100 transformation steps are shown in Figures 18 and 19, respectively.

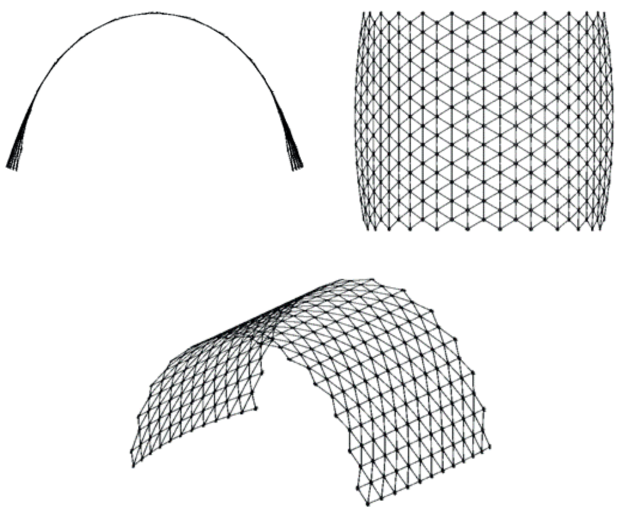

Figure 18. Visualization of the shape change after 50 displacement steps along the X-axis

The plots of changes $\Delta l / l$ in the rods of the lattice at 50 and 100 transformation steps are presented in Fig. 20. As can be seen from the plots in Figs. 11 and 20, the numerical values of extreme longitudinal strains in the rods of the considered hexagonal and rectangular regular lattices at 50 transformation steps practically coincide. In both schemes, the greatest longitudinal tensile strains are experienced by the contour nodes subjected to kinematic boundary conditions.

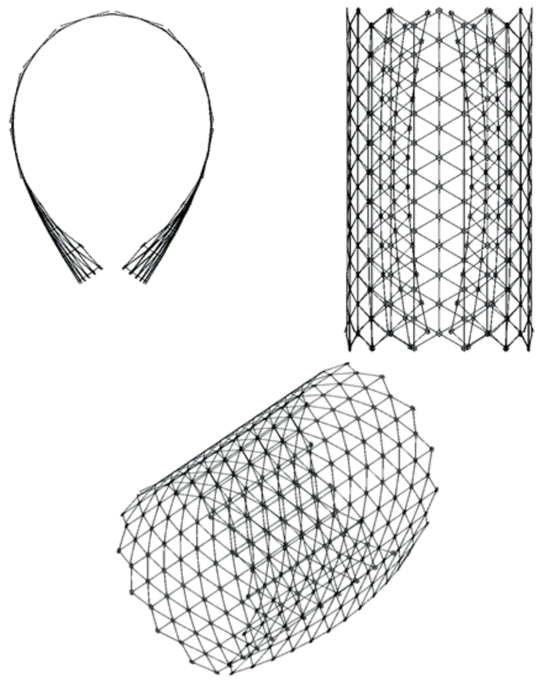

Figure 19. Visualization of the shape change after 100 displacement steps along the X-axis

It should be noted that the rectangular lattice (Fig. 19) has the greatest ability to change its shape; it practically rolls up into a "roll" at 100 transformation steps.

In order to investigate the influence of the scheme of kinematic boundary conditions on the transformation process of a rectangular lattice, we consider a two-sided scheme of discrete displacements at all nodes with coordinates $x = 0$ and $x = 10.48$ m. Visualization of the lattice pattern after 50 steps at $\Delta_x = 0.5$ m is shown in Fig. 21.

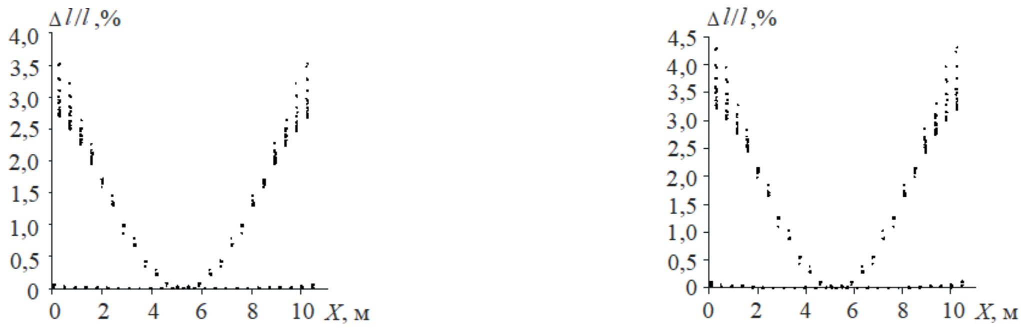

a *b*

Figure 20. Plots of the change $\Delta l / l$ in the rods at displacement of contour nodes along the X axis: a - 50 steps; b - 100 steps

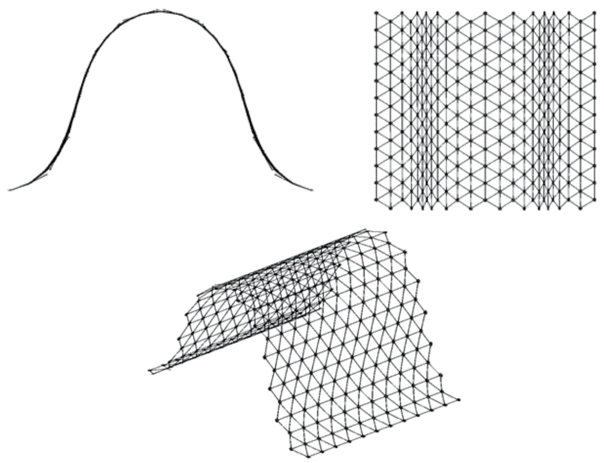

Figure 21. Visualization of lattice change after 50 displacement steps along the X-axis at two-sided discrete displacement

The plot of $\Delta l / l$ for a two-sided discrete displacement of the contour nodes is shown in Figure 22

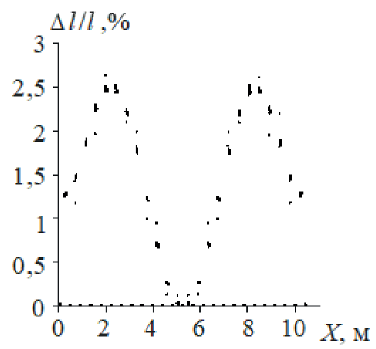

Figure 22. Plots of the change in the rods at a two-sided discrete displacement

It can be seen from the graph in Fig. 22 that the maximum tensile longitudinal strains at the two-sided discrete displacement of the contour nodes appear in the rods located in the kink areas.

CONCLUSIONS

1. A method of finite element modeling of transformation of a regular rod system from a flat to a dome-shaped state by discrete displacement of contour nodes of the lattice is proposed.
2. As a criterion limiting the process of the structure shape change, the values of longitudinal strains of the rods are proposed to be used.

REFERENCES

1. **D.P. Perrin and C.E. Smith.**(2001) Rethinking classical internal forces for active contour models, in 2013 IEEE Conference on Computer Vision and Pattern Recognition, vol.3, pp. 615. doi: 10.1109/CVPR.2001.991020.
2. **Kass M., Witkin A., Terzopoulos D. Snakes** (1988) Active contour models. Int J Comput Vision, vol.1, pp. 321–331.
3. **McInerney T, Terzopoulos D.** (1996) Deformable models in medical image analysis: a survey, Medical Image Analysis, vol. 1, no. 2, pp. 91-108. doi:10.1016/S1361-8415(96)80007-7.
4. **Terzopoulos D., Fleischer K.** (1988) Deformable models, The Visual Computer 4, pp. 306–331.

5. **Terzopoulos D., Platt J., Barr A., Fleischer K.** (1987). Elastically Deformable Models. ACM Siggraph Computer Graphics, vol.21.
6. **Miller J., Breen D., Lorensen W., O'Bara R., Wozny M.** (1991) Geometrically deformed models. ACM SIGGRAPH Computer Graphics, vol.25, pp. 217-226.
7. **McInerney, T., Terzopoulos, D.** (1995). A dynamic finite element surface model for segmentation and tracking in multidimensional medical images with application to cardiac 4D image analysis. Computerized medical imaging and graphics : the official journal of the Computerized Medical Imaging Society, vol.19 1, pp. 69-83.
8. **Terzopoulos D., Witkin A., Kass M.,** (1988). Constraints on Deformable Models: Recovering 3D Shape and Nonrigid Motion, Artificial Intelligence, vol.36, pp. 91-123.
9. **Popov V., Sorokin F.** (2017) Development of the final element of a flexible rod with separate storage of accumulated and additional rotations for modeling large movements of structural elements of aircraft. Proceedings of MAI, vol. 92, pp. 3. (in Russian).
10. **Battini J.M. (**2002) Co-rotational beam elements with warping effects in instability problems. Computer Methods in Applied Mechanics and Engineering, vol. 191, no. 17-18, P pp. 1755-1789.
11. **Nizametdinov F., Sorokin F.** (2018) Features of the application of the Euler vector to describe large turns in the modeling of structural elements of aircraft using the example of a rod finite element. Proceedings of MAI, vo.l 102, no. 1. (in Russian).
12. ANSYS Mechanical APDL Programmers Reference. Reference. Release 15.0ANSYS, Inc. http://www.ansys.com
13. **Gaydzhurov P., Tsaritova N., Kurbanov A., Kurbanova A., Iskhakova E.** (2022). Numerical simulation of the process of directed transformation of a regular hinge-rod system. International Journal for Computational Civil and Structural Engineering, vol. 18(3), pp.14–24. https://doi.org/10.22337/2587-9618-2022-18-3-14-24.
14. **Gaydzhurov P., Iskhakova E., Savelieva N., Tsaritova N.** (2020). Finite element modeling of the shaping process of a hinge-rod system under controlled kinematic action. News of higher educational institutions. The North Caucasus region. Technical sciences, vol.3 (207), pp. 5-12.
15. **Perelmuter A.V., Kabantsev O.V.** (2015). Analysis of structures with a changing calculation scheme. Moscow: SCUD SOFT Publishing House, DIA Publishing House,. 148 p.

СПИСОК ЛИТЕРАТУРЫ

1. **D.P. Perrin and C.E. Smith**.(2001) Rethinking classical internal forces for active contour models, in 2013 IEEE Conference on Computer Vision and Pattern Recognition, vol.3, pp. 615. doi: 10.1109/CVPR.2001.991020.
2. **Kass M., Witkin A., Terzopoulos D. Snakes** (1988) Active contour models. Int J Comput Vision, vol.1, pp. 321–331.
3. **McInerney T, Terzopoulos D.** (1996) Deformable models in medical image analysis: a survey, Medical Image Analysis, vol. 1, no. 2, pp. 91-108. doi:10.1016/S1361-8415(96)80007-7.
4. **Terzopoulos D., Fleischer K.** (1988) Deformable models, The Visual Computer 4, pp. 306–331.
5. **Terzopoulos D., Platt J., Barr A., Fleischer K.** (1987). Elastically Deformable Models. ACM Siggraph Computer Graphics, vol.21.
6. **Miller J., Breen D., Lorensen W., O'Bara R., Wozny M.** (1991) Geometrically deformed models. ACM SIGGRAPH Computer Graphics, vol.25, pp. 217-226.
7. **McInerney, T., Terzopoulos, D.** (1995). A dynamic finite element surface model for segmentation and tracking in multidimensional medical images with

application to cardiac 4D image analysis. Computerized medical imaging and graphics : the official journal of the Computerized Medical Imaging Society, vol.19 1, pp. 69-83.
8. **Terzopoulos D., Witkin A., Kass M.,** (1988). Constraints on Deformable Models: Recovering 3D Shape and Nonrigid Motion, Artificial Intelligence, vol.36, pp. 91-123.
9. **Попов В.В., Сорокин Ф.Д.** (2017) Разработка конечного элемента гибкого стержня с раздельным хранением накопленных и дополнительных вращений для моделирования больших перемещений конструктивных элементов летательных аппаратов. Труды МАИ, № 92, с. 3.
10. **Battini J.M. (**2002) Co-rotational beam elements with warping effects in instability problems. Computer Methods in Applied Mechanics and Engineering, vol. 191, no. 17-18, P pp. 1755-1789.
11. **Низаметдинов Ф.Р., Сорокин Ф.Д.** (2018). Особенности применения вектора эйлера для описания больших поворотов при моделировании элементов конструкций летательных аппаратов на примере стержневого конечного элемента. Труды МАИ, (102), с. 1.
12. ANSYS Mechanical APDL Programmers Reference. Reference. Release 15.0ANSYS, Inc. http://www.ansys.com
13. **Gaydzhurov P., Tsaritova N., Kurbanov A., Kurbanova A., Iskhakova E.** (2022). Numerical simulation of the process of directed transformation of a regular hinge-rod system. International Journal for Computational Civil and Structural Engineering, vol. 18(3), pp.14–24. https://doi.org/10.22337/2587-9618-2022-18-3-14-24.
14. **Гайджуров П.П., Исхакова Э.Р., Савельева Н.А., Царитова Н.Г.** (2020). Конечно-элементное моделирование процесса формоизменения шарнирно-стержневой системы при управляемом кинематическом воздействии. Известия высших учебных заведений. Северо-Кавказский регион. Технические науки, № 3 (207), с.5-12.
15. **Перельмутер А.В., Кабанцев О.В.** Анализ конструкций с изменяющейся расчетной схемой. М.: Издательство СКАД СОФТ, Издательский дом АСВ, 2015. 148 с.

Peter P. Gaydzhurov, PhD, DSc, Professor of the Department «Technical mechanics», Don State Technical University, Rostov-on-Don, Advisor to the Russian Academy of Architecture and Building Sciences
e-mail: gpp-161@yandex.ru

Nadezhda G. Tsaritova, PhD, Associate Professor of the Department «Urban development, designing of buildings and structures», Platov South-Russian State Polytechnic University, (NPI), Novocherkassk,
e-mail: ncaritova@yandex.ru

Гайджуров Петр Павлович, доктор технических наук, профессор кафедры «Техническая механика» Донского государственного технического университета, советник РААСН, г. Ростов-на-Дону, e-mail: gpp-161@yandex.ru

Царитова Надежда Геннадьевна, кандидат технических наук, доцент кафедры «Градостроительство, проектирование зданий и сооружений», Южно-Российского государственного политехнического университета им. М.И.Платова (НПИ), г. Новочеркасск. e-mail: ncaritova@yandex.ru